Metal Organic Frameworks for Bioelectrochemical Applications

Bernhard Auer, Shane Telfer, Andrew James Gross

Metal Organic Frameworks for Bioelectrochemical Applications

Bernhard Auer[2], Shane G. Telfer[2], A. J. Gross[1]*

[1] Department of Molecular Chemistry, Univ. Grenoble Alpes, CNRS, 38000 Grenoble, France. Email: andrew.gross@univ-grenoble-alpes.fr
[2] MacDiarmid Institute for Advanced Materials and Nanotechnology, School of Natural Sciences, Massey University, Palmerston North, New Zealand.

Keywords: MOFs, bioelectrocatalysis, electrochemical sensors, biofuel cells, biocomposites

Abstract

Metal organic frameworks (MOFs) with their high pore volumes and chemically-diverse pore environments have emerged as components of catalytic electrodes for biosensors, biofuel cells, and bioreactors. MOFs are widely exploited for gas capture, separations, and catalysis, but their integration at electrodes with biocatalysts for (bio)electrocatalysis is a niche topic that remains largely unexplored. This review focuses on recent advances in MOF and MOF-derived carbon electrodes for bioelectrochemical applications. A range of MOF materials and their integration into devices with enzymes and microbes are reported. Key properties and performance characteristics are considered and opportunities facing MOFs for (bio)electrochemical applications are discussed.

1. Introduction to MOFs for bioelectrochemistry

Metal organic frameworks (MOFs) are crystalline, porous materials resembling "molecular sponges" formed by the self-assembly of organic linkers and metal ions or clusters. Owing to their high surface areas and pore volumes and chemical tunability, MOFs have attracted tremendous attention for gas adsorption and separation[1,2], energy storage[3], and catalysis[4]. Crystalline and amorphous MOFs are typically obtained by solvothermal and hydrothermal reactions between organic linker precursors and metal salts in water or high boiling point organic solvents. Microwave-assisted synthesis methods are also popular since they can provide access to enhancements in yield, purity and efficiency, as well as shorter reactions times. Solvothermal and hydrothermal reaction times vary from a few hours to days while microwave-assisted methods can provide products in minutes. MOF synthesis requires careful control of parameters including temperature, counter ions, reactant concentration, solvent, structure-directing agents and modulators. Over the last few years, MOF-enzyme composites have attracted interest for biocatalysis[5]. This often takes advantage of the protective roles of MOFs that can enhance catalytic activity, efficiency, reusability, and/or stability vis-à-vis native enzymes[5,6]. MOFs and MOF-derived materials have also recently gained attention for electrocatalysis[7,8]. Recent years have also seen the emergence of electrically-conductive MOFs, for example, prepared through incorporation of mixed valence metals or conjugated redox-active organic units[8]. MOF-derived materials include porous carbons, metal oxides, and their composites. In this review, we focus on the niche research topic where MOFs and MOF-derived materials, including carbons formed by pyrolysis, are combined with electrodes and enzymes or microbes and explored for applications in bioelectrochemistry.

Enzymes and other essential biocatalytic components such as redox mediators and cofactors are typically integrated with MOFs either (a) *in-situ* ("*de novo*") during MOF synthesis from the precursor metal salt and ligands, or (b) by post-functionalisation of already synthesised MOFs on surfaces or in solution[5]. For the "*de novo*" strategy, the biocatalysts are introduced into the pores of the MOF by co-precipitation or biomineralisation methods which integrate the synthesis of MOFs and biocatalyst encapsulation in one step[9]. Entrapment of biocatalysts such as enzymes with sizes of ca. 3-10 nm occurs via suitably large mesopores that feature in the MOF structure. Pore entrapment can bring advantages such as (i) reduced leaching via chemical interactions and/or size-exclusion effects, and (ii) enhanced stability, for example, by preventing enzyme unfolding, limiting catalyst aggregation, or by shielding the catalyst from chemical attack[5,6]. Wu et al. showed that pore-encapsulated glucose oxidase (GOx) prepared via co-precipitation in amorphous zeolitic imidazolate frameworks (ZIFs) exhibited a five-fold higher chemical stability to protease digestion and a 2-30 fold higher thermal stability at 55-80 ºC compared to the free enzyme[10]. Zhou and coworkers showed that encapsulated catalase and superoxide dismutase in mesoporous nanocomposites improved catalytic activity compared to the free enzyme in the presence of inhibiting proteases and at a wide range of pH values[11]. Such results open up perspectives for applications in bioelectrochemistry given that such oxidoreductases are widely used in this domain[12,13]. Enzymatic activity and stability studies, including recycling and leaching assays, and BET surface analysis before and after enzyme immobilisation, are used to confirm effective enzyme encapsulation in MOF materials. UV-visible spectroscopy enzyme assays and/or direct analysis of characteristic absorption features (e.g. the Soret band) may be used to quantify the amount of enzyme encapsulated[6,10,11]. Pore sizes including pore apertures must of course be carefully considered and compatible with the size of the enzyme. Spectroscopic techniques such as Raman spectroscopy and solid-state NMR have been effectively employed to further understand enzyme confinement, for example, to observe specific MOF-enzyme interactions[14].

For applications in bioelectrochemistry, it is necessary to use MOFs that provide the necessary stability in aqueous solutions from buffers to complex biofluids. Several reports have evaluated MOF stability in aqueous solutions[5,15,16]. Unfortunately, due to the lability of ligand-metal bonds, many MOFs are sensitive to hydrolysis. However, promising MOFs for aqueous bioelectrochemistry, based on reported stability and BET surface area studies, are highlighted in Fig. 1. Azolate frameworks including the archetypal imidazolate framework, ZIF-8, as well as ZIF-67 and triazolate-based MAF-7, have shown excellent hydrolytic stabilities and performance under harsh conditions, depending on factors such as buffer type, pH and crystallite size[15,17]. For example, Tris and HEPES buffers proved compatible with ZIF-8 (bio)materials[18,19]. Zn-based ZIF-8 is currently the most widely used MOF for the preparation of MOF-enzyme composites[5,18]. Zr-based carboxylate MOFs including the exemplary UiO-66 are also commonly considered for aqueous use[20]. In a benchmark robustness study, UiO-66 proved stable in water, even more so than ZIF-8, and stable at both acidic and neutral pH[15]. Metal-carboxylate MIL MOFs such as MIL-100, as well as related structures like MIL-101 and MIL-53, are also popular with their large pores and chemical stability, for example, showing hydrothermal stability[20,22,23]. Milner and coworkers highlighted that Fe- and Cr-based MIL-100 are generally stable to acidic, neutral, and harshly oxidising conditions[15]. MIL-100(Cr) showed the best stability of 17 MOFs tested under acidic conditions. MIL-101(Cr) and MIL-100(Fe) remained intact after exposure to boiling water for seven days. MIL-53(Al) exhibited hydrolytic stability in HEPES buffer and proved to be highly resistant to hydrolysis in neutral and acidic solutions for 7 days[22,24,25]. Salicylate frameworks

including MOF-74(Ni) tolerated deionised water as well as phosphate and Tris buffers at pH 7, and basic conditions, but degraded at pH 1[15]. Zr-pyrene-based mesoporous channel MOFs such as NU-1006 are also of interest with proven stability in bis-tris-propane (BTP) buffer at pH 7.2[26]. Such MOFs may be considered generally appropriate for bioelectrochemical applications although stability is best evaluated on a case-by-case basis. MOF stability should be evaluated based on powder x-ray diffraction (PXRD) and electron microscopy data as well as, where possible, ligands/metal ion leaching and porosity and gas adsorption experiments[27].

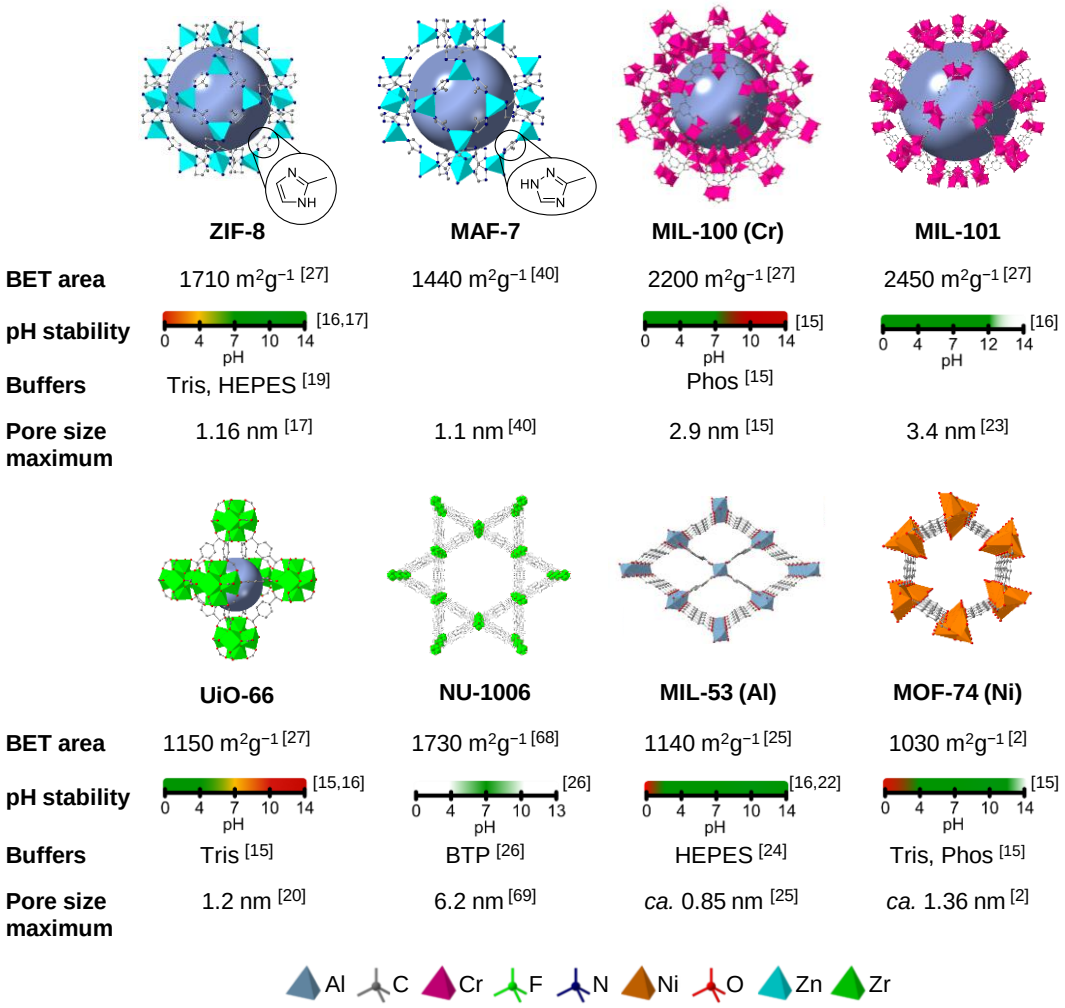

Fig. 1: Water-stable MOFs in various aqueous solutions based on data typically obtained after at least 24 h immersion in solution and involving PXRD analysis. pH stability bar (crystallinity): retained (green), partial loss (yellow), significant loss (red).

2. MOFs for biological fuel cells

Biofuel cells that exploit enzymes or microbes as biocatalysts to generate electrical energy offer an eco-friendly energy solution for powering electronic devices[28,29]. Enzymatic biofuel cells are promising for low-power applications such as portable medical devices[30] while microbial biofuel

cells are better suited for larger scale applications such as energy-generating wastewater treatment systems[31]. Biofuel cells generate power from bioelectrochemical reactions via the oxidation of fuels such as glucose, at the (bio)anode, coupled with the reduction of oxidants, such as oxygen, at the (bio)cathode[29,32]. Biofuel cells are nevertheless typically hampered by limitations including the limited stability and activity of the biocatalysts and their bioelectrode interfaces, particularly under challenging real world conditions.

2.1. Enzymatic biofuel cells

An appealing use of MOFs for bioelectrochemical applications is as a precursor for carbon frameworks with exquisite porosities and improved electrical conductivity. Jiang et al. reported in 2017 the first biofuel cell that exploited MOFs[33]. Rather than use the pristine MOF, the ZIF-8- was pyrolysed to give hollow tubular carbon. A glucose/O_2 biofuel cell was developed comprising a GOx bioanode, prepared using the MOF-derived carbon, coupled with a Pt-based cathode. A high catalytic current of 2.1 mA cm^{-2} at 0.5 V vs. SCE was observed in 0.1 M phosphate buffer (PB) pH 7. The biofuel cell delivered a practical open circuit voltage (OCV) of 0.63 V and power output of 310 µW cm^{-2} with 110 mmol L^{-1} glucose. The power performance was superior to the hybrid biofuel previously reported by the same team that used an N-doped tubular carbon in place of the MOF-derived carbon[34]. The carbonisation temperature of 600 °C used is low which likely limited the graphitic content and in turn electrical conductivity of the MOF-derived carbon. The use of a higher pyrolysis temperature of 910 °C to obtain ZIF-8 derived carbons was explored by Xiao and coworkers[35]. A series of micro/mesoporous ZIF-8-like cobalt-nitrogen-carbon (Co-N-C) materials were obtained then used to construct O_2-reducing cathodes. The reported biofuel with the MOF-derived cathode and a GOx bioanode produced an OCV of 0.34 V and a low power output of 3.9 µW cm^{-2} in 0.1 M PB pH 7 with only 5 $mmol^{-1}$ glucose. The onset potential for O_2 reduction at the cathode was about 300 mV less positive compared to a bilirubin oxidase (BOx) biocathode, at least partially explaining the low OCV and power observed.

Some progress has been made on the use of MOFs for enzyme encapsulation for bioelectrochemical applications. In 2020, Wei and coworkers explored the first complete enzymatic biofuel cell exploiting MOFs, and notably, exploited *in-situ* enzyme encapsulation[36]. In an unusual setup, a ZIF-8/laccase composite used at both the anode and cathode. A low OCV of 0.197 V and very low power output of 0.04 mW cm^{-2} was achieved, limited by the high potential of the cathode half-cell reaction. Nevertheless, remarkable improvements in catalytic activity were observed for the encapsulated enzyme composite vs. the free enzyme at high temperature and in organic solvents. A six-fold higher activity remained after 2 h at 70 ºC while a two-fold higher activity remained after 20 days storage in organic solvent[36]. Wei and coworkers very recently expanded the use of ZIF-8 laccase composites for the preparation of a stretchable biofuel cell that delivered stable power during stretching and a power maximum of 1.33 W m^{-3}[37]. Enzyme encapsulation was also explored for the preparation of ZIF-8 laccase and ZIF-8 GOx composites[38]. GOx replaced laccase at the bioanode while the nanofibers based on cellulose improved biocompatibility. The biofuel cell produced up to 0.4 mW cm^{-3} and an OCV of 0.35 V with 10 $mmol^{-1}$ glucose. The power performance is low compared to other glucose/O_2 biofuel cells[32,39]. Yimamumaimaiti et al. explored enzyme encapsulation and reported extremely promising results using MAF-7[40]. MAF-7 is isoreticular to ZIF-8 but can offer improved mechanical properties, hydrophilicity, and improved enzyme protection in denaturing conditions[40,41]. A glucose/O_2 biofuel cell was developed that incorporated a MAF-7-

GOx/horseradish peroxidase (HRP) composite interlaced with single walled carbon nanotubes (SWCNTs) together with a simple BOx cathode[40]. A maximum power output of 119 µW cm^{-2} with an OCV of ca. 0.34 V was achieved in human blood compared to only 14 µW and a ca. 0.22 V OCV when MAF-7 was not incorporated. The performance compares well to the benchmark study of Mano and coworkers[42]. The MAF-7 composite also showed enhanced stability at 65 ºC and in the presence of organic solvents (Fig. 2).

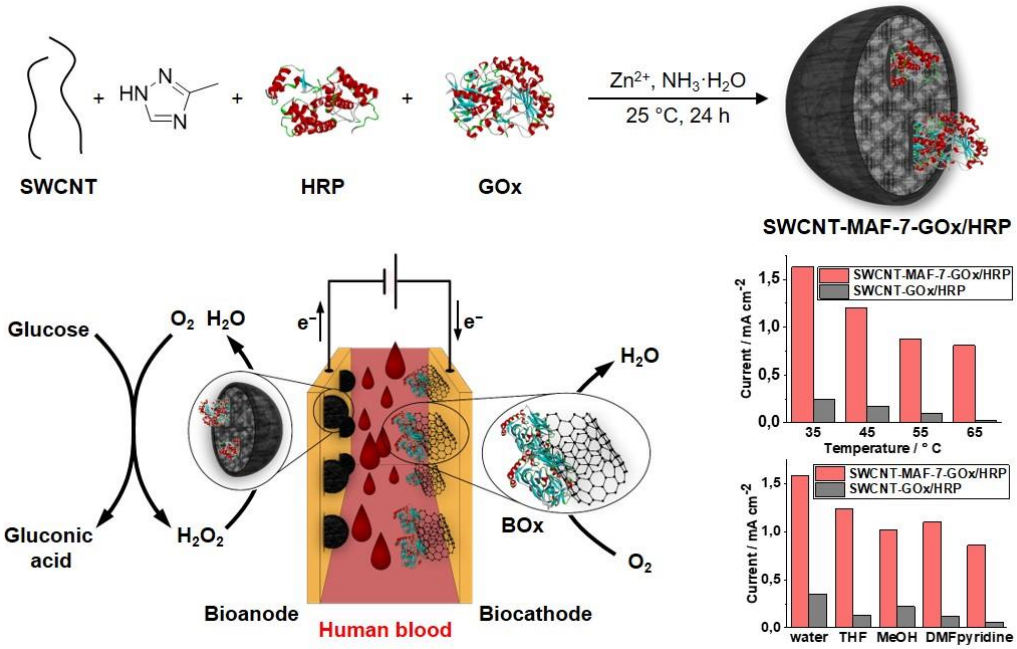

Fig. 2: Blood tolerating glucose/O_2 enzymatic biofuel cell exploiting SWCNT-MAF-7-GOx/HRP bioanode. Image adapted from ref. [40]. Graphs illustrate catalytic glucose oxidation current vs. temperature or media type.

Encapsulation of a redox mediator (electron relay) rather than the enzyme has also been explored for the construction of an enzymatic biocathode[43]. Redox mediators are essential for effective mediated electron transfer (MET) bioelectrocatalysis involving enzymes such as GOx, laccase or BOx. Leaching of biocatalytic components including redox mediators from electrode interfaces is a commonly encountered issue. Stennou, Serre and coworkers developed a laccase-based cathode that used mesoporous Fe-based MIL-100 with encapsulated (2,2'-azino-bis(3-ethylbenzothiazoline-6-sulfonic acid)) (ABTS). The ABTS mediator, commonly exploited for multicopper oxidases, was encapsulated in the mesopores of the framework as well as in the bulk structure. The MOF-ABTS biocomposite cathode showed only a negligible loss of mediator after 5 days in 0.1 M acetate buffer pH 5.1; a very promising result. A mediated bioelectrocatalytic reduction of O_2 was achieved although the maximum current density was low (34 µA cm^{-2}) at ca. 0.15 V *vs.* AgAgCl. The same strategy could eventually be expanded to other types of redox mediators or even enzyme cofactors. Li and coworkers explored the encapsulation of redox molecules in an unusual setup[44]. ZIF-8/$[Fe(CN)_6]^{3-}$ nanocarriers were used in a "smart" pH responsive biofuel cell. An FAD-dependent glucose (FADGDH) bioanode was coupled with a ferricyanide-based redox cathode. The biofuel cell operated on the basis that $[Fe(CN)_6]^{3-}$ was reduced after being released in-situ via acid degradation of ZIF-8. The biofuel cell delivered a low

power output of 23 µW cm^{-2}, a reasonable OCV of 0.38 V, and negligible performance loss after 20 days. The same team reported a more powerful "smart" biofuel cell that combined a ZIF-8 FADGDH bioanode with a UiO-66-NH_2/$[Fe(CN)_6]^{3-}$ cathode[45]. The biofuel cell delivered a higher power density of 619 µW cm^{-2}, an improved OCV of 0.46 V, and 30 day stability in Tris HCl buffer pH 7.4 with 25 mmol L^{-1} glucose. The advantage of using pendant –NH_2 groups on the UiO-66 was not clearly demonstrated but provides interesting perspectives e.g. for coupling of enzymes and other biocatalytic components to the MOF structure.

2.2 Microbial biofuel cells

MOFs have also been explored for use in microbial biofuel cells. Microbial biofuel cells generate energy via microbial oxidation of organic substrates at the anode combined with an oxygen-reducing cathode. The use of MOFs in microbial biofuel cells is almost entirely limited to the preparation of MOF-based cathodes for the electrocatalytic O_2 reduction reaction (ORR) rather than for bioelectrocatalytic reactions. At the time of writing, to the best of our knowledge, there is only one example where MOFs were used to construct a microbial bioanode[46]. In 2021, Xu et al. revealed how Fe-based MIL-53, and particularly MIL-53-NH_2, enhanced active anaerobic bacterial growth and adhesion as well as electron transfer between exoelectrogens and the electrode. Attractive bioelectrocatalytic currents up to *ca.* 14 mA cm^{-2} at 0.5 V vs. AgAgCl were achieved compared to ≤ 2.5 mA cm^{-2} for an equivalent bioanode without the MOF. Keitz and coworkers earlier showed how Fe-based MOFs such as MIL-100 can support the growth and even enhance the redox activity of metal-reducing bacteria with the MOF acting as a high surface area respiratory substrate[47].

Several advances have been made on the development of pristine MOFs and MOF-derived carbons for the construction of ORR cathodes and their use in microbial biofuel cells. MOF-derived cobalt catalysts have been prepared by pyrolysis of ZIF-67 to yield CoNC materials with high microporosity that performed better than pristine ZIF-67 for the ORR reaction at neutral pH[48]. In a microbial biofuel cell setup, the MOF-derived carbon improved resistance to undesirable biofilm formation compared to the classical Pt/C electrode (Fig. 3).

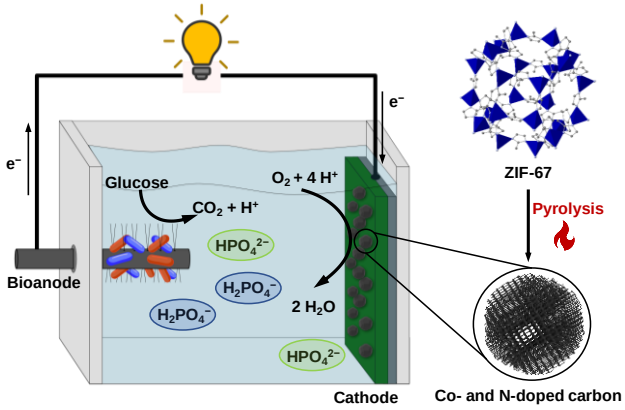

Fig. 3: Single chamber microbial biofuel cell integrating a ZIF-67-derived Co- and N-doped carbon cathode. Image adapted from ref. [48].

Another strategy to further improve such materials is to incorporate a metal salt in the MOF prior to pyrolysis. This approach is used to introduce catalytic metal sites as well as enhance the

graphitisation and conductivity[49]. Metal-doped CoNC was used in a microbial biofuel cell with a glucose-fed bacterial bioanode that operated for at least 755 h and delivered a maximum power density of 4336 mW m^{-2} at ca. 0.5 V at neutral pH; the highest power to date for a microbial biofuel cell integrating MOFs. The biofuel with the MOF-derived cathode exhibited considerably more power compared to the benchmark Pt/C cathode (2521 mW m^{-2}). The use of CoNC derived from UiO-66 appears less promising; performance was not improved compared to the Pt/C cathode[50]. Li and coworkers shed new light on the influence of pyrolysis temperature on the conductivity and catalytic activity of FeCoNC MOF-derived materials. For example, pyrolysis at 900 °C maximised mesopore content[51]. Such mesoporous materials could be exploited to facilitate mass transport in microbial bioelectrodes or even for enzyme entrapment. The acetate-fed biofuel cell performed better with the MOF-derived cathode than with the Pt/C cathode, in part, due to improved resistance to microbial biofouling. MOF-derived FeCoS cathodes are also promising. Yan et al. showed the possibility to deliver 2.55 times more power with such MOF-derived cathodes compared to an equivalent cell setup employing a Pt/C cathode (862 mW m^{-2} vs. 334 mW m^{-2}) in wastewater[52]. Improved resistance to sulfur-related pollutants (S^{2-} and SCN^{-}) and therefore improved stability over 350 h was also reported compared to the Pt/C cathode.

The use of pristine MOFs as opposed to MOF-derived carbons in microbial biofuel cells has also been reported. In 2020, UiO-66 was exploited in a catalytic ink deposited on a carbon felt cathode[53]. Higher catalytic currents were observed when using UiO-66 rather than Pt/C. Power performance and water treatment efficiency of the microbial biofuel cell was however similar for both. The main advantage of the UiO-66 cathode is that it provides a 4-fold cost advantage compared to Pt/C (2.09 mW/$US vs. 0.47 mW/$US). Xue et al. reported a 2-fold higher catalytic current when using a ZIF-8 cathode compared to the Pt/C for the cathode[54]. The biofuel cell exhibited a maximum power density of 2103 mW m^{-2} and was operated for 110 h, representing a 60% improvement compared to the benchmark Pt/C. The same authors also reported an ORR cathode based on carbonised ZIF-67 which offers the main advantage of improved stability[51].

3. Enzyme-based electrochemical biosensors

Enzymatic bioelectrodes have attracted considerable attention for rapid and quantitative detection of a plethora of organic analytes[55]. Enzymatic bioelectrodes employing GOx or GDH electrodes for blood glucose sensing have already shown remarkable commercial success for diabetes management. Ongoing challenges are to develop bioelectrodes capable of sensitive and selective detection in complex media and, ideally, continuous monitoring over periods of months. The materials used should be, as far as possible, biocompatible and biodegradable. Pristine MOFs and MOF-derived functional materials have been reviewed recently as promising candidates for electrochemical sensing[56]. In this section of the review we focus specifically on MOFs that have been used for *enzyme-based* electrochemical sensing.

The first enzyme-based electrochemical biosensors that incorporated MOFs were reported in 2013 in a breakthrough study by Mao and coworkers[57]. NAD-dependent GDH and ZIF nanocrystals were adsorbed at a carbon electrode. ZIF-70 provided the best overall adsorption capacity and therefore loading for both the enzyme and its redox mediator (methylene green). Impressively, the amperometric glucose sensor at 0 V vs. AgAgCl functioned effectively for real-time monitoring in cerebral biofluid at physiologically-relevant concentrations (0.1 to 2 mmol L^{-1}) and for at least 100 min.

Beyond simple enzyme adsorption, Singh and coworkers explored enzyme encapsulation via biomineralisation with the objective of improving enzyme stabilisation as well as nanoconfinement effects. A single-step method was developed for the encapsulation of three different enzymes for glucose biosensing[58]. In one example, a ZIF-8/GOx composite adsorbed at a MWCNTs electrode facilitated ultra-stable amperometric detection at -0.05 V vs. AgAgCl at physiological concentrations (1-10 mmol L^{-1}) with a limit of detection (LOD) of 50 µmol L^{-1} in Tris buffer (Fig. 4). Improved thermal stability up to 70 °C was also observed, further validating the efficacy of enzyme encapsulation in bulk mesopores. Li et al. also developed ZIF-8/GOx bioelectrodes via an enzyme encapsulation protocol[38]. Rather than simple amperometric detection, the authors developed a self-powered glucose biosensor based on a biofuel cell setup comprising a glucose bioanode coupled with a ZIF-8/laccase O_2-reducing biocathode[38]. The concentration-dependent OCV output of the biofuel cell was exploited as the sensor and permitted detection over the physiological range (1-20 mmol L^{-1}) with an LOD of ca. 5 µmol L^{-1}. Continuous monitoring was demonstrated for 15 h in acetate buffer pH 4.5. Patra et al. developed GOx-based glucose biosensors using MOFs but employed MIL-100 and MIL-127 rather than ZIF-8[59]. The Fe-based MIL-100 with cavities of 2.5 nm and 2.9 nm was combined with GOx on a Pt electrode. Amperometric glucose detection was demonstrated with a high sensitivity (71 mA M^{-1} cm^{-2}), LOD of 5 µmol L^{-1}, and a fast response time (< 5 s) in acetate buffer pH 5.3. Enhanced stability up to 90% and 78% after 21 days under wet and dry conditions, respectively, was observed, compared to the control sensor prepared without MIL-100.

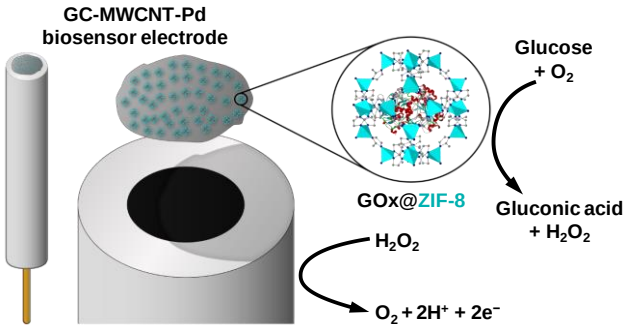

Fig. 4: Electrochemical biosensor exploiting a GOx-ZIF-8 nanocomposite prepared via biomineralisation. Image adapted from ref. [58].

A small number of MOF-based electrochemical biosensors have also been developed for the detection of toxic contaminants such as bisphenols[36,60,61], chlorpyrifos[62], and paraoxon[63]. The first biosensors for bisphenol detection employed a Cu-based MOF with a paddle-wheel structure to enhance tyrosinase adsorption at the MOF surface[60,61]. Sensor transduction was based on the electrochemical reduction of the o-diquinone formed via the tyrosinase-catalysed oxidation of the bisphenol. The CuMOF/tyrosinase biosensor exhibited a low onset potential of -0.1 V vs. AgAgCl in phosphate buffer; the low potential minimised electrochemical interferences[61]. A wide detection range (0.05-3 µmol L^{-1}), a low LOD, larger catalytic currents, and two-fold higher sensitivity (224 mA M^{-1}) were observed when the CuMOF was used, in part due to increased enzyme and analyte adsorption. The same authors also comprehensively studied the responses of 9 BPA analogues in the presence of heavy metals, demonstrating robust detection in industrial metal-containing wastewaters[60]. A self-powered sensor for bisphenol A detection has also been

developed based on a ZIF-8/laccase composite anode for BPA oxidation coupled with a laccase only O_2-reducing cathode[36]. In contrast to the self-powered glucose sensor that used OCV for signal transduction[37], here the sensor used the concentration-dependent power output as the sensor signal. A linear detection range of 10-400 µmol L^{-1} and an LOD of 1.95 µmol L^{-1} was reported.

In 2019, Nagabooshanam reported a portable microelectrode biosensor for organophosphate pesticide detection[62]. MOF Basolite® W1200 (ZIF-8) was used as a host matrix to increase enzyme loading with a view to enhancing chlorpyrifos detection. The sensor relies on the electrochemical oxidation of thiocholine generated enzymatically via hydrolysis of acetylthiocholine. The concentration-dependent inhibition of the enzyme by chlorpyrifos was used as the sensor signal. The sensor met EU detection requirements with a detection range of 10-100 ng L^{-1} and an LOD of 6 ng L^{-1} in 0.1 M PB at pH 7. Vegetable sample analysis with excellent recoveries as well as 20-day stability was demonstrated. Wei et al. also used the acetylcholinesterase inhibition strategy but for detection of the pesticide, paraoxon[64]. A MOF (Fe-BTC)-derived carbon was obtained by thermal decomposition then used as a host matrix to promote acetylcholinesterase adsorption. The linear range of the sensor was 0.1 pmol L^{-1} to 100 nmol L^{-1}. A low LOD of 0.12 pm was achieved. Acceptable reproducibility, one-month stability with only 7% signal loss, and good recoveries in tap water were demonstrated. Bagheri and coworkers also developed an inhibition-based biosensor using acetylcholinesterase for paraoxon detection[63]. UiO-66 was selected not only for its stability and porosity but also for the possibility to replace Zr sites with $Ce^{3+/4+}$ electron relays. Ce also introduced oxophilicity that enhanced enzyme and analyte adsorption. Good reproducibility, 20 day stability, and good selectivity in the presence of non-organophosphates was reported but the performance appears less promising compared to the Fe-BTC derived carbon biosensor[64].

MOF-based electrochemical biosensors that use cytochrome C (Cyt C) protein have been developed for H_2O_2 and 3-MCPD detection. Ge and coworkers developed an original mesoporous-templated ZIF-8 (mesoZIF-8) for Cyt C encapsulation to facilitate H_2O_2 sensing[65]. The encapsulated redox protein exhibited increased activity, affinity and stability compared to the native enzyme. Furthermore, no protein leakage was observed after 1-week storage in buffer compared to almost complete leakage after 1.5 days for the protein adsorbed at classical ZIF. The mesoZIF-8/Cyt C composite was also resistant to 80 ºC at 1 h. The sensor strategy relied on the amperometric reduction of enzymatically oxidised H_2O_2 at -0.05 V vs. AgAgCl. The linear detection range was ca. 0.1-3.6 mmol L^{-1} and the sensor performed satisfactorily for food sample analysis. He et al. also used Cyt C for electrochemical biosensing but this time for detection of the food contaminant, 3-MPCD, via protein-mediated electrochemical oxidation[66]. An Fe-based MOF was used to increase enzyme loading and stability compared to the classical electrode. Voltammetric sensing was linear from 2-100 mg L^{-1} and the LOD was 0.41 mg L^{-1}.

To the best of our knowledge, there is only one example where MOF-derived (graphitised) carbons have been used to construct electrochemical enzymatic biosensors[67]. In this work, a hierarchical porous carbon was formed by pyrolysis of IRMOF-8 at 1000 °C in an inert atmosphere. The porous MOF-derived carbon played a role as the electrocatalyst for NADH oxidation as well as host for the NAD^+-dependent alcohol dehydrogenase. The authors demonstrated voltammetric detection of ethanol in the range of 10-300 mmol L^{-1}, a sensitivity of 24 nA mmol L^{-1}, and an LOD of 3 mmol L^{-1}. The bioelectrode also showed good stability, maintaining 80% of its catalytic signal after 14 days at 20°C. The hierarchical structure improved the immobilisation of electrically-wired enzymes, facilitated electrolyte and analyte mass

transport, and increased the conductivity and specific surface areas, overall, resulting in a superior catalytic current than that obtained when only MWCNTs were used as the support.

4. Enzymatic bioreactors

The combination of electrochemistry with enzymes provides access to the high selectivity and reaction rates of enzymes as well as the ability to use electrochemistry for cofactor regeneration or controlled cosubstrate supply and/or production[68]. An important global challenge concerns the reduction of CO_2 emissions with eventually the possibility to convert CO_2 into value-added products. In 2019, Farha and coworkers developed an electroenzymatic reactor that combined the mesoporous MOF, NU-1006, with encapsulated NAD-dependent formate dehydrogenase (NAD-FDH) and a Rh complex on an indium tin oxide (ITO) electrode (Fig. 5)[69]. The MOF with 6.2 nm mesopores permitted effective enzyme encapsulation based on adsorption experiments and theoretical calculations. The Rh complex facilitated electroreduction of enzymatically formed NAD^+ to the enzyme's substrate, NADH. After 1 h at -1.1 V, CO_2 was effectively transformed into 25 mmol of formic acid (turnover number = 1.3×10^4). The enzymatic activity was 3-fold higher following enzyme encapsulation in the MOF.

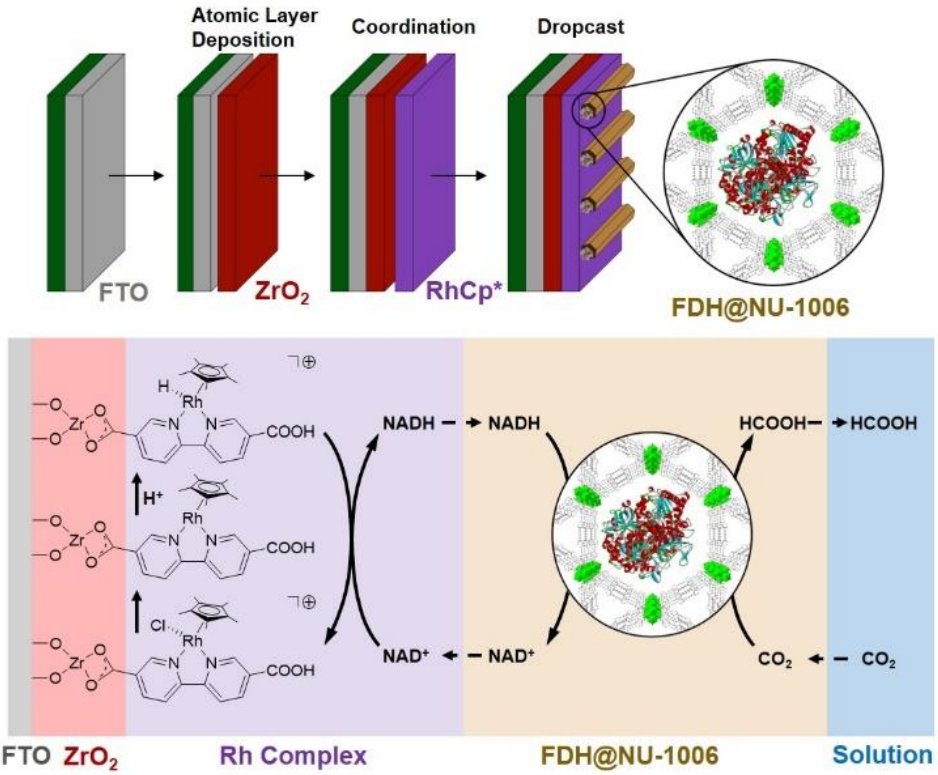

Fig. 5: Enzymatic reactor for bioelectrocatalytic reduction of CO2 with high efficiency exploiting NU-1006 with encapsulated formate dehydrogenase. Image adapted from ref. [69].

Very recently, an elegant cascade-type electroenzymatic reactor was developed with ZIF-8 encapsulated enzymes (NAD-FDH, formaldehyde GDH, and alcohol GDH) to convert CO_2 into

methanol via formaldehyde[70]. Enzymes were effectively loaded with ca. 93% efficiency. After 3 h at -0.7 V, 0.742 mmol of methanol was produced whereas only 0.061 mmol of methanol was produced with the free enzymes. The advantages of using ZIF-8 in this case included the higher local concentration of adsorbed CO_2 (302 mmol) compared to the CO_2 solubility limit in water (33 mmol), and the ability to promote NAD^+ adsorption. The authors also show stability advantages in Tris buffer pH 7.4 where the residual activity of encapsulated enzymes was 51 % while the activity of the free enzymes was reduced to 25 %.

5. Conclusion

In recent years, the development of MOFs and their (bio)composites for the elaboration of enzymatic bioelectrodes has resulted in substantial developments, not only in electrochemistry and bioelectrocatalysis, but also in the fields of porous materials science and inorganic chemistry. In this review we have shown how researchers have incorporated biocatalytic components such as enzymes, proteins, redox molecules, and microbes, in MOF and MOF-derived and templated carbons, to enhance enzymatic, electrocatalytic, and bioelectrocatalytic reactions at electrode interfaces. It is clear that MOFs can provide protection and nanoconfinement effects, or simply be used as supporting matrices to enhance the loading of biocatalytic components. MOFs can also be used as templates to obtain highly conductive, stable and even electrocatalytic porous carbons with intrinsic sites for reactions such as NADH oxidation or O_2 reduction. MOFs have also been used as biodegradable carriers or as biocompatible substrates to promote bacterial growth and adhesion. The ability of MOFs to enhance the solubility and accumulation of substrates such as CO_2 and bisphenol A for (bio)electrocatalytic reactions is another important advantage that can be exploited for biosynthesis or sensing, and perhaps eventually, for energy conversion. Many untapped opportunities remain, ranging from the development and application of MOFs and MOF-derived materials with large mesopores, or with redox-active or conjugated systems to enhance the conductivity or even selectivity of MOF layers. Such systems promise to facilitate bioelectrocatalytic reactions, for example, by improving electron transfer rates and/or mass transport. Further theoretical and experimental studies will be necessary to better understand biocatalyst encapsulation, the effects of pore sizes on mass transport, as well as stability, degradation, and cytotoxicity in aqueous environments, towards the overarching further improvement of bioelectrochemical devices.

References

[1] O. T. Qazvini, R. Babarao, S. G. Telfer, *Nat. Commun.* **2021**, *12*, 197.
[2] H. Wu, W. Zhou, T. Yildirim, *J. Am. Chem. Soc.* **2009**, *131*, 4995.
[3] G. Xu, P. Nie, H. Dou, B. Ding, L. Li, X. Zhang, *Mater. Today* **2017**, *20*, 191.
[4] A. Bavykina, N. Kolobov, I. S. Khan, J. A. Bau, A. Ramirez, J. Gascon, *Chem. Rev.* **2020**, *120*, 8468.
[5] X. Lian, Y. Fang, E. Joseph, Q. Wang, J. Li, S. Banerjee, C. Lollar, X. Wang, H.-C. Zhou, *Chem. Soc. Rev.* **2017**, *46*, 3386.
[6] D. Feng, T.-F. Liu, J. Su, M. Bosch, Z. Wei, W. Wan, D. Yuan, Y.-P. Chen, X. Wang, K. Wang, X. Lian, Z.-Y. Gu, J. Park, X. Zou, H.-C. Zhou, *Nat. Commun.* **2015**, *6*, 5979.
[7] W. Zheng, L. Y. S. Lee, *ACS Energy Lett.* **2021**, *6*, 2838.
[8] L. S. Xie, G. Skorupskii, M. Dinca, *Chem. Rev.* **2020**, *120*, 8536.

[9] S. S. Nadar, L. Vaidya, V. K. Rathod, *Int. J. Biol. Macromol.* **2020**, *149*, 861.
[10] X. Wu, H. Yue, Y. Zhang, X. Gao, X. Li, L. Wang, Y. Cao, M. Hou, H. An, L. Zhang, S. Li, J. Ma, H. Lin, Y. Fu, H. Gu, W. Lou, W. Wei, R. N. Zare, J. Ge, *Nat. Commun.* **2019**, *10*, 5165.
[11] X. Lian, A. Erazo-Oliveras, J.-P. Pellois, H.-C. Zhou, *Nat. Commun.* **2017**, *8*, 2075.
[12] C. Abreu, Y. Nedellec, A. J. Gross, O. Ondel, F. Buret, A. L. Goff, M. Holzinger, S. Cosnier, *ACS Appl. Mater. Interfaces* **2017**, *9*, 23836.
[13] E.-H. Yoo, S.-Y. Lee, *Sensors* **2010**, *10*, 4558.
[14] W. Yang, W. Liang, L. A. O'Dell, H. D. Toop, N. Maddigan, X. Zhang, A. Kochubei, C. Doonan, Y. Jiang, J. Huang, *JACS Au 2021, 1,* 2172.
[15] Z. Wang, A. Bilegsaikhan, R. T. Jerozal, T. A. Pitt, P. J. Milner, *ACS Appl. Mater. Interfaces* **2021**, *13*, 17517.
[16] K. Leus, T. Bogaerts, J. De Decker, H. Depauw, K. Hendrickx, H. Vrielinck, V. Van Speybroeck, P. Van Der Voort, *Microporous Mesoporous Mater.* **2016**, *226*, 110.
[17] K. S. Park, Z. Ni, A. P. Côté, J. Y. Choi, R. Huang, F. J. Uribe-Romo, H. K. Chae, M. O'Keeffe, O. M. Yaghi, *Proc. Natl. Acad. Sci.* **2006**, *103*, 10186.
[18] Y. Gao, C. M. Doherty, X. Mulet, *ChemistrySelect* **2020**, *5*, 13766.
[19] M. A. Luzuriaga, C. E. Benjamin, M. W. Gaertner, H. Lee, F. C. Herbert, S. Mallick, J. J. Gassensmith, *Supramol. Chem.* **2019**, *31*, 485.
[20] J. Winarta, B. Shan, S. M. Mcintyre, L. Ye, C. Wang, J. Liu, B. Mu, *Cryst. Growth Des.* **2020**, *20,* 1347.
[21] Y.-K. Seo, J. W. Yoon, J. S. Lee, Y. K. Hwang, C.-H. Jun, J.-S. Chang, S. Wuttke, P. Bazin, A. Vimont, M. Daturi, S. Bourrelly, P. L. Llewellyn, P. Horcajada, C. Serre, G. Férey, *Adv. Mater.* **2012**, *24*, 806.
[22] X. Qian, B. Yadian, R. Wu, Y. Long, K. Zhou, B. Zhu, Y. Huang, *Int. J. Hydrog. Energy* **2013**, *38*, 16710.
[23] G. Férey, C. Mellot-Drazieks, C. Serre, F. Millange, J. Dutour, S. Surblé, I. Margiolaki, *Science* **2005,** *309,* 2040.
[24] S. Nandi, E. Sharma, V. Trivedi, S. Biswas, *Inorg. Chem.* **2018**, *57*, 15149.
[25] T. Loiseau, C. Serre, C. Huguenard, G. Fink, F. Taulelle, M. Henry, T. Bataille, G. Férey, *Chem. – Eur. J.* **2004**, *10*, 1373.
[26] P. Li, Q. Chen, T. C. Wang, N. A. Vermeulen, B. L. Mehdi, A. Dohnalkova, N. D. Browning, D. Shen, R. Anderson, D. A. Gómez-Gualdrón, F. M. Cetin, J. Jagiello, A. M. Asiri, J. F. Stoddart, O. K. Farha, *Chem* **2018**, *4*, 1022.
[27] J. Osterrieth, *ChemRxiv* **2022**, DOI 10.26434/chemrxiv-2022-8rhph-v3.
[28] A. Gross, M. Holzinger, S. Cosnier, *Energy Env. Sci* **2018**, *11*, 1670.
[29] C. Santoro, C. Arbizzani, B. Erable, I. Ieropoulos, *J. Power Sources* **2017**, *356*, 225.
[30] P. Bollella, I. Lee, D. Blaauw, E. Katz, *ChemPhysChem* **2020**, *21*, 120.
[31] Y. Guo, J. Wang, S. Shinde, X. Wang, Y. Li, Y. Dai, J. Ren, P. Zhang, X. Liu, *RSC Adv.* **2020**, *10*, 25874.
[32] S. Cosnier, A. J. Gross, A. Le Goff, M. Holzinger, *J. Power Sources* **2016**, *325*, 252.
[33] K. Jiang, X. Zhang, J. Huang, S. Wang, J. Chen, *J. Electroanal. Chem.* **2017**, *796*, 88.
[34] W. Wang, K. Jiang, X. Zhang, J. Chen, *RSC Adv.* **2016**, *6*, 29142.
[35] X. Feng, X. Xiao, J. Zhang, L. Guo, Y. Xiong, *Electrochim. Acta* **2021**, 138791.
[36] X. Li, D. Li, Y. Zhang, P. Lv, Q. Feng, Q. Wei, *Nano Energy* **2020**, *68*, 104308.

[37] X. Li, Q. Feng, D. Wu, A. Mensah, W. Li, Y. Cai, D. Li, Q. Wei, *Mater. Today Energy* **2021**, *22*, 100886.
[38] X. Li, Q. Feng, K. Lu, J. Huang, Y. Zhang, Y. Hou, H. Qiao, D. Li, Q. Wei, *Biosens. Bioelectron.* **2021**, *171*, 112690.
[39] A. J. Gross, X. Chen, F. Giroud, C. Abreu, A. Le Goff, M. Holzinger, S. Cosnier, *ACS Catal.* **2017**, *7*, 4408
[40] T. Yimamumaimaiti, X. Lu, J.-R. Zhang, L. Wang, J.-J. Zhu, *ACS Appl. Mater. Interfaces* **2020**, *12*, 41429.
[41] W. Liang, H. Xu, F. Carraro, N. K. Maddigan, Q. Li, S. G. Bell, D. M. Huang, A. Tarzia, M. B. Solomon, H. Amenitsch, L. Vaccari, C. J. Sumby, P. Falcaro, C. J. Doonan, *J. Am. Chem. Soc.* **2019**, *141*, 2348.
[42] M. Cadet, S. Gounel, C. Stines-Chaumeil, X. Brilland, J. Rouhana, F. Louerat, N. Mano, *Biosens. Bioelectron.* **2016**, *83*, 60.
[43] S. Patra, S. Sene, C. Mousty, C. Serre, A. Chaussé, L. Legrand, N. Steunou, *ACS Appl. Mater. Interfaces* **2016**, *8*, 20012.
[44] P. Gai, C. Gu, X. Kong, F. Li, *iScience* **2020**, *23*, 101133.
[45] C. Gu, L. Bai, L. Pu, P. Gai, F. Li, *Biosens. Bioelectron.* **2021**, *176*, 112907.
[46] H. Xu, J. Huang, C. Lin, J. Zheng, Z. Qiu, Q. Wen, Y. Chen, L. Qi, Y. Wang, *Electrochim. Acta* **2021**, *368*, 137622.
[47] S. K. Springthorpe, C. M. Dundas, B. K. Keitz, *Nat. Commun.* **2019**, *10*, 5212.
[48] S. You, X. Gong, W. Wang, D. Qi, X. Wang, X. Chen, N. Ren, *Adv. Energy Mater.* **2016**, *6*, 1501497.
[49] H. Tang, S. Cai, S. Xie, Z. Wang, Y. Tong, M. Pan, X. Lu, *Adv. Sci.* **2016**, *3*, 1500265.
[50] K. Zhong, L. Huang, M. Li, Y. Dai, Y. Wang, J. Zuo, H. Zhang, B. Zhang, S. Yang, J. Tang, J. Yan, M. Su, *Int. J. Hydrog. Energy* **2019**, *44*, 30127.
[51] W. Xue, Q. Zhou, F. Li, *Electrochim. Acta* **2020**, *355*, 136775.
[52] Y. Yan, Y. Hou, Z. Yu, L. Tu, S. Qin, G. Yuan, D. Lan, S. Chen, J. Sun, S. Wang, *J. Power Sources* **2020**, *472*, 228582.
[53] I. Das, Md. T. Noori, M. Shaikh, M. M. Ghangrekar, R. Ananthakrishnan, *ACS Appl. Energy Mater.* **2020**, *3*, 3512.
[54] W. Xue, Q. Zhou, F. Li, B. S. Ondon, *J. Power Sources* **2019**, *423*, 9.
[55] T. Monteiro, M. G. Almeida, *Crit. Rev. Anal. Chem.* **2019**, *49*, 44.
[56] C.-H. Chuang, C.-W. Kung, *Electroanalysis* **2020**, *32*, 1885.
[57] W. Ma, Q. Jiang, P. Yu, L. Yang, L. Mao, *Anal. Chem.* **2013**, *85*, 7550.
[58] R. Singh, M. Musameh, Y. Gao, B. Ozcelik, X. Mulet, C. M. Doherty, *J. Mater. Chem. C* **2021**, *9*, 7677.
[59] S. Patra, T. H. Crespo, A. Permyakova, C. Sicard, C. Serre, A. Chaussé, N. Steunou, L. Legrand, *J. Mater. Chem. B* **2015**, *3*, 8983.
[60] X. Lu, X. Wang, L. Wu, L. Wu, Dhanjai, L. Fu, Y. Gao, J. Chen, *ACS Appl. Mater. Interfaces* **2016**, *8*, 16533.
[61] X. Wang, X. Lu, L. Wu, J. Chen, *Biosens. Bioelectron.* **2015**, *65*, 295.
[62] S. Nagabooshanam, S. Roy, A. Mathur, I. Mukherjee, S. Krishnamurthy, L. M. Bharadwaj, *Sci. Rep.* **2019**, *9*, 19862.
[63] E. Mahmoudi, H. Fakhri, A. Hajian, A. Afkhami, H. Bagheri, *Bioelectrochemistry* **2019**, *130*, 107348.
[64] W. Wei, S. Dong, G. Huang, Q. Xie, T. Huang, *Sens. Actuators B Chem.* **2018**, *260*, 189.

[65] C. Zhang, X. Wang, M. Hou, X. Li, X. Wu, J. Ge, *ACS Appl. Mater. Interfaces* **2017**, *9*, 13831.
[66] B. He, L. Wang, M. Li, *J. Iran. Chem. Soc.* **2021**, *18*, 151.
[67] F. Zhang, X. Wu, J. Gao, Y. Chen, Y. Gui, L. Zhang, W. Gan, Q. Yuan, *Electrochim. Acta* **2020**, *340*, 135958.
[68] C. Kohlmann, W. Märkle, S. Lütz, *J. Mol. Catal. B Enzym.* **2008**, *51*, 57.
[69] Y. Chen, P. Li, H. Noh, C.-W. Kung, C. T. Buru, X. Wang, X. Zhang, O. K. Farha, *Angew. Chem. Int. Ed.* **2019**, *58*, 7682.
[70] Z. Zhang, J. Li, M. Ji, Y. Liu, N. Wang, X. Zhang, S. Zhang, X. Ji, *Green Chem.* **2021**, *23*, 2362.